D6.2 Report on testing OEF and extending earthquake forecasts to loss forecasts in Italy

Deliverable information	
Work package	WP6
Lead	UNINA
Authors	E. Chioccarelli A. Pacifico I. Iervolino
Reviewers	H. Crowley, EUCENTRE
Approval	Management Board
Status	Final
Dissemination level	Public
Delivery deadline	28.02.2023
Submission date	11.04.2023
Intranet path	[DOCUMENTS/DELIVERABLES/File Name]

Table of contents

Summary

MANTIS v2.0 is an operational earthquake loss forecasting (OELF) system developed for Italy during the RISE project. It provides seismic risk metrics (e.g., the expected values of collapsed buildings) at the municipality scale, combining, via a consistent approach, forecasted weekly seismic hazard rates, vulnerability, and inventory models. The seismic hazard rates refer to a grid of point-like seismic sources covering the whole national area and some sea; they are computed by the Italian operational earthquake forecasting system (named OEF-Italy) that provides the expected number of earthquakes exceeding magnitude four, in the week following the analysis. The adopted vulnerability models are the state-dependent fragility functions that were computed, for defined structural typologies, during the same research project. Finally, inventory models collect information, at the municipality scale, about the number of buildings in each structural typology. The aim of this document is to demonstrate the operationalization of the system, which was one of the objectives of RISE. Thus, after recalling the main features of the system and the models involved in its implementation, this deliverable provides MANTIS v2.0 results retrospectively computed during the Central Italy 2016 seismic sequence.

1.   Introduction

OEF-Italy (Marzocchi et al., 2014) is the name of the Italian system for operational earthquake forecasting (OEF) that allows to constantly update the short time estimates of seismicity in a region in which the earthquake activity is continuously monitored (Jordan et al., 2011). On the basis of data provided by OEF-Italy, a system for extending to loss measures the seismic forecasts was developed (Iervolino et al., 2015). Such a system, identified as operational earthquake loss forecasting (OELF) and named MANTIS-K, combines the weekly seismicity rates with vulnerability and inventory models for the Italian building stock to obtain weekly forecasts of seismic risk (consequences) metrics, that is, the expected number of collapsed buildings, fatalities, injuries, and displaced residents.

MANTIS-K has some limitations that may affect the accuracy of the loss forecasting. The system adopts vulnerability and inventory models that do not change in time, that is, OEF rates are the only input that change among the loss forecasting computed at different times. This does not appear as an issue in peace conditions (i.e., when no earthquake has recently occurred in the area), but it may affect results right after the occurrence of a damaging earthquake (i.e., during a seismic crisis). Thus, an upgraded version of the system, named MANTIS v2.0, was developed in the context of the RISE project as described in Chioccarelli et al. (2023). Indeed, MANTIS v2.0 is able to provide loss forecasting accounting for the structural damage accumulation due to the occurred (damaging) earthquakes. An example of results of MANTIS v2.0 was already provided in the cited document, referring to the seismic sequence of L'Aquila that occurred in 2009 and computed by the work-in-progress formulation of MANTIS v2.0. In the same document, a comparison between results of MANTIS-K and MANTIS v2.0 was discussed. Hereafter, the main characteristics of MANTIS v2.0 are first recalled. Then, the results of the final completely implemented version of MANTIS v2.0 during the long-lasting seismic sequence of Central Italy in 2016 are discussed.

2.   Main characteristics of MANTIS v2.0

The upgraded version of the OELF system is formulated to account for the evolution, over time, of the structural damage conditions. This implies that loss forecasting must account for the possible structural damage accumulation due to the occurrence of more than one earthquake in the forecasting period. Moreover, the upgraded system has to estimate the possible damage due to the occurred earthquakes and, consequently, forecast the performance level of buildings that, at the time of computation, are already at an intermediate performance level. In the following, the

loss forecasting referring to a building inventory constituted by already damaged buildings is discussed first. Then, the way in which MANTIS v2.0 can account for (i) the possible structural damage accumulation due to the occurrence of more than one earthquake in the forecasting time window and (ii) the inventory update due to the structural damage evolution in the sequence are briefly described.

2.1   Loss forecasting referring to already damaged buildings

In order to account for damage accumulation, some hypotheses about the structural damage evolution over time have to be introduced. More specifically, it is assumed that, for each building of the considered structural typology, the probability to pass from pl_i with $i=1,...,n-1$ to another (worse) performance level, pl_j with $i<j\leq n$, due to one earthquake does not depend on the damage history of the structure, but it only depends on pl_i and on the intensity of the earthquake possibly causing the transition, that is im. This enables adopting a Markov-chain model, in analogy with (Iervolino et al., 2016), to compute the probability that a structure, located at the $\{w,z\}$ site, passes from pl_i to pl_j $(j>i)$ given the occurrence of a *generic* earthquake (an earthquake of unspecified magnitude and location), indicated as $P_{i,j}^k(t,w,z)$, is computed as per Eq. (1):

$$P_{i,j}^k(t,w,z)=$$
$$=\sum_{q=1}^{Q}P[\theta_q]\cdot\int_{im=0}^{+\infty}P[PL^k=pl_j|pl_i,im]\cdot\iint_{x\,y}\frac{\lambda(t,x,y)}{\nu(t,w,z)}\cdot\int_{m=0}^{+\infty}f_{IM|M,R,\theta}(im|m,r,\theta_q)\cdot f_M(m)\cdot dm\cdot dx\cdot dy\cdot d(im) \tag{1}$$

In the equation, $\lambda(t,x,y)$ is the expected number per unit time (Δt, equal to one week) of earthquakes above magnitude four, originating at the point-like seismic sources $\{x,y\}$ (it is provided by OEF-Italy); M is the magnitude of the earthquake, R is the distance between the point-like seismic source $\{x,y\}$ and the site of interest $\{w,z\}$; $f_M(m)$ is the probability density function (pdf) of the magnitude of the earthquakes (assumed to be independent and identically distributed among sources); $f_{IM|M,R,\theta}(m,r,\theta)$ is the pdf of the intensity measure, IM, at the site $\{w,z\}$ conditional to $M=m$, $R=r$, and the soil class θ (or possibly other covariates); $P[PL^k=pl_j|pl_i,im]$ is the probability the structure makes a transition from pl_i to pl_j for a given value of IM. The latter can be evaluated as the difference between two probabilities, both conditional on the value of the intensity measure and the performance level pl_i in which the structure is before the earthquake occurrence; such conditional probabilities are those of reaching or exceeding pl_j and pl_{j+1}, respectively and are defined as state-dependent fragility functions. Finally, $\lambda(t,x,y)/\nu(t,w,z)$ is the probability that, given that an earthquake affects the $\{w,z\}$ site, it is generated by the $\{x,y\}$ source; $\nu(t,w,z)$ is the rate of the earthquakes affecting the $\{w,z\}$ site and can be computed as shown in Eq. (2):

$$\nu(t,w,z)=\iint_{x\,y}\lambda(t,x,y)\cdot dx\cdot dy . \tag{2}$$

A matrix collecting all the transition probabilities of the same structural typology at $\{w,z\}$ site given the occurrence of an earthquake, $[P^k(t,w,z)]$, can be defined as in Eq. (3) (for the sake of simplicity, the dependency on $\{w,z\}$ and time is neglected for the terms within the matrix):

$$[P^k(t,w,z)]=\begin{bmatrix} 1-\sum_{j=2}^{n}P_{1,j}^k & P_{1,2}^k & \cdots & \cdots & P_{1,n}^k \\ 0 & 1-\sum_{j=3}^{n}P_{2,j}^k & \cdots & \cdots & P_{2,n}^k \\ \cdots & \cdots & \cdots & \cdots & \cdots \\ 0 & \cdots & 0 & 1-P_{(n-1),n}^k & P_{(n-1),n}^k \\ 0 & \cdots & \cdots & 0 & 1 \end{bmatrix} . \tag{3}$$

The matrix has $n \times n$ dimension and the element at row i and column j is the probability that, due to a generic earthquake, one structure of the k-th typology, that is in pl_i before the earthquake, goes to pl_j due to the earthquake occurrence. Thus, $\left[P^k(t,w,z) \right]$ is an upper triangular matrix because the structure cannot lower its performance level due to an earthquake occurrence.

The unit time transition probability matrix for the structural typology, $\left[P_E^k(t,t+\Delta t,w,z) \right]$, collecting the transition probabilities from one damage state to another in Δt, can be computed. Assuming that, in the unit time, the process of earthquake occurrence can be approximated by a homogeneous Poisson Process, HPP, (in analogy with what was discussed for MANTIS-K), if $\nu(t,w,z)$ is small (i.e., the probability of more than one earthquake in Δt is negligible), the matrix $\left[P_E^k(t,t+\Delta t,w,z) \right]$ can be approximated via Eq. (4):

$$\left[P_E^k(t,t+\Delta t,w,z) \right] \approx \nu(t,w,z) \cdot \left[P^k(t,w,z) \right] + \left\{ 1 - \nu(t,w,z) \right\} \cdot [I], \tag{4}$$

where $\nu(t,w,z)$ approximates the probability of one earthquake occurrence in the unit time, $\left\{ 1 - \nu(t,w,z) \right\}$ approximates the probability of no earthquake in the unit time and $[I]$, the identity matrix, accounts for the fact that, when no earthquake occurs, the building does not change its performance level.

Once $\left[P_E^k(t,t+\Delta t,w,z) \right]$ is known, the expected number of buildings in each damage state at time $(t+\Delta t)$ can be computed knowing the number of buildings in each damage state at time t. More specifically, let us assume that $\mathbf{N}_B^k(t,w,z)$ is the vector collecting the number of the buildings of the k-th structural typology located in $\{w,z\}$ at the time t, the expected number of buildings in each performance level at $(t+\Delta t)$, $\mathbf{N}_B^k(t+\Delta t,w,z)$, is provided by as:

$$\mathbf{N}_B^k(t,w,z) \cdot \left[P_E^k(t,t+\Delta t,w,z) \right] = \left\{ N_{B,pl_1}^k(t,w,z), N_{B,pl_2}^k(t,w,z),...,N_{B,pl_n}^k(t,w,z) \right\} \cdot \left[P_E^k(t,t+\Delta t,w,z) \right]. \tag{5}$$

Indeed, in Eq. (5), the transition probabilities from a starting damage state to an arriving one are multiplied by the corresponding number of buildings in the starting damage state.

2.2 Loss forecasting accounting for more than one earthquake

Depending on the seismic history, the rates of OEF may result in a value of $\nu(t,w,z)$ that corresponds to a non-negligible probability of more than one earthquake in Δt. In this case, the approximation introduced in Eq. (4) is not acceptable, but the application of the described Markovian approach remains possible if the original unit time, i.e. one week, is partitioned into smaller intervals such that, in each of them, the probability of more than one earthquake is negligible. Thus, the way in which the original Δt has to be partitioned depends on the distribution of the number of expected earthquakes over time. Once the length of the new time intervals is defined, Eq. (4) can be applied for each of them and the transition probability matrix referred to one week can be computed proofing of the Markov-chain properties. The resulting transition probability matrix will account for the possible damage accumulation due to multiple forecasted earthquakes in one week.

2.3 Inventory update

After the occurrence of each earthquake, it is important to update the $\mathbf{N}_B^k(t,w,z)$ vector to apply Eq. (5). To this aim, MANTIS v2.0, before each computation, checks if a new ShakeMap was delivered by the INGV website (http://shakemap.ingv.it/shake4/) and, if any, retrieves the available data, making use of the INGV web services. The downloaded ShakeMaps are combined with the state-dependent fragility curves via the procedure described in Chioccarelli et al. (2023), to estimate the level of structural damage produced by the occurred earthquakes. With such information, the vector collecting the estimated number of buildings in each damage state, $\mathbf{N}_B^k(t,w,z)$, is updated and adopted in Eq. (5) as an input value for the operational earthquake loss forecasting as discussed in Section 2.1.

3.   CASE STUDY

In this deliverable, Central Italy, 2016, seismic sequence (e.g., Iervolino et al., 2017; Luzi et al., 2017) is retrospectively analysed by means of MANTIS v2.0. The characteristics of the seismic sequence are described hereafter together with the models adopted for MANTIS v2.0 implementation. The discussion of results is reported in Section 4.

The first significant earthquake occurred at 1:36 on the 24/08/2016. It was characterized by a moment magnitude (M) equal to 6 and it was followed by a sequence of earthquakes that, until the end of October, showed a lower magnitude. Indeed, the M6 was considered as the mainshock of the sequence for several weeks until, at 06:40 on the 30/10/2016, a M6.5 earthquake occurred. The significant length of sequence and the occurrence of several earthquakes of significant magnitude, makes the sequence particularly interesting for the application of MANTIS v2.0.

In the following, the results of MANTIS v2.0 are reported after each OEF release that was preceded by the occurrence of one (or more) earthquakes with M equal to or larger than 4.5 (it is preliminarily assumed that earthquakes with magnitude lower than 4.5 produced negligible damage to the existing buildings). More specifically, the first column of Table 1 shows the OEF release to which MANTIS v2.0 results refer. In the same table, the M4.5+ earthquakes that occurred before the OEF release are reported from column 2 to 6: the ID of the ShakeMaps adopted for updating the building portfolio is reported in column 2, the magnitude, the time, and the epicentre coordinates are reported in columns from 3 to 6, respectively.

Table 1. Considered OEF releases and M4.5+ events that occurred during the Central Italy seismic sequence.

OEF Release	ShakeMap ID	M	Time	Latitude [°]	Longitude [°]
24/08/2016 02:00	7073711	6	01:36	42.71	13.23
	7073641	4.5	01:37	42.71	13.25
24/08/2016 02:45	7076161	5.4	02:33	42.79	13.15
24/08/2016 12:45	7105011	4.5	11:30	42.82	13.16
26/08/2016 04:45	7224451	4.8	04:28	42.60	13.29
26/10/2016 17:30	8663031	5.4	17:10	48.87	13.12
	8663041	4.5	17.11	42.88	13.13
26/10/2016 19:30	8669361	4.5	19:17	42.90	13.13
	8669321	5.9	19:18	42.90	13.09
26/10/2016 21:45	8676191	4.5	21:42	42.86	13.12
30/10/2016 07:00	8863681	6.5	06:40	42.83	13.11
30/10/2016 12:15	8882341	4.5	12:07	42.84	13.07

3.1   Implemented models

The short-term hazard modelling relies on the OEF-Italy forecasted rates $\lambda(t,x,y)$. The numerical values of the OEF rates, released by OEF-Italy and listed in Table 1, are represented from **Error! Reference source not found.** to Figure 9. The sum of the OEF rates for the point-like seismic sources within 70km from the epicenter of the mainshock are reported in Figure 10.

For each point-like seismic source, the pdf of the generated magnitude, $f_M(m)$, is derived from the Gutenberg–Richter relationship (Gutenberg & Richter, 1944) with unbounded maximum magnitude and b-value equal to one. At the site of interest $\{w,z\}$, the conditional distribution of the intensity measure $f_{IM|M,R,\theta_q}\left(im|m,r,\theta_q\right)$ is computed using the ground motion prediction equation (GMPE) of (Bindi et al., 2011).

To be consistent with the fragility models (described in the next section), the geometric mean of the pseudo-spectral accelerations, $Sa(T)$, over a range of spectral periods is chosen as intensity measure (Baker & Cornell, 2006). Such an intensity measure, denoted as $Sa_{avg}(\mathbf{T})$, is defined by Eq. (6):

$$Sa_{avg}(\mathbf{T}) = \sqrt[L]{\prod_{l=1}^{L} Sa(T_l)}, \tag{6}$$

The vector $\mathbf{T}$ collects the twenty-three vibration periods considered in Bindi et al. (2011) GMPE: T={0, 0.04, 0.07, 0.1, 0.15, 0.2, 0.25, 0.3, 0.35, 0.4, 0.45, 0.5, 0.6, 0.7, 0.8, 0.9, 1, 1.25, 1.5, 1.75, 2, 2.5, 2.75}s, where $Sa(0s)$ represents the peak ground acceleration or PGA.
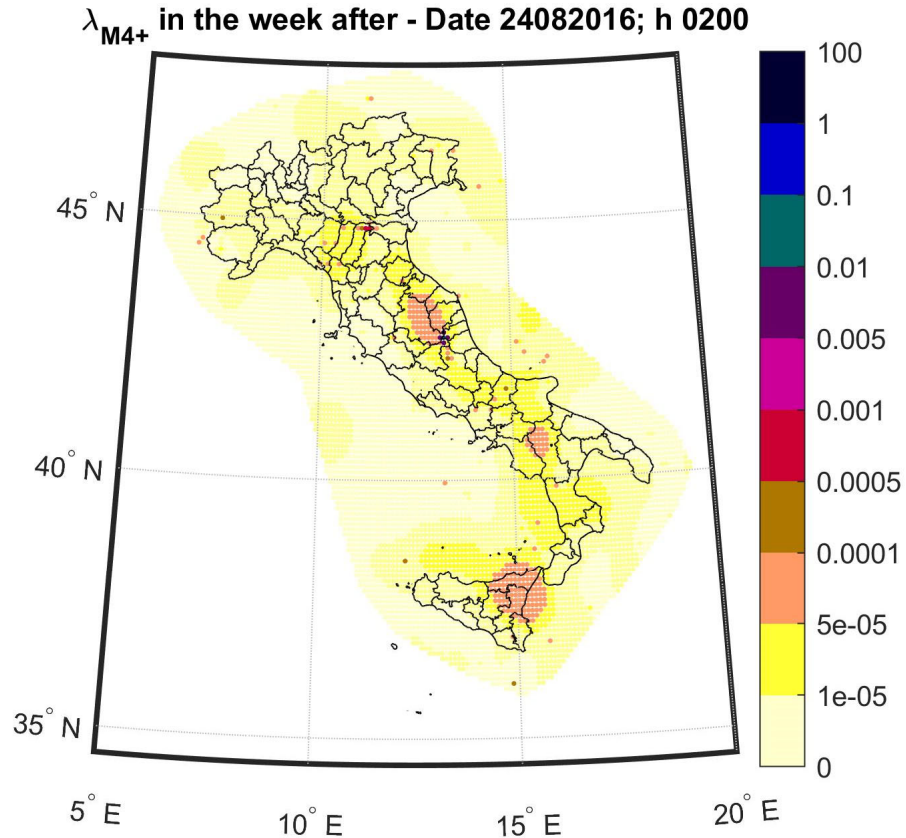
Figure 1. Weekly rates from OEF-Italy weekly at 24/08/2016, 02:00.
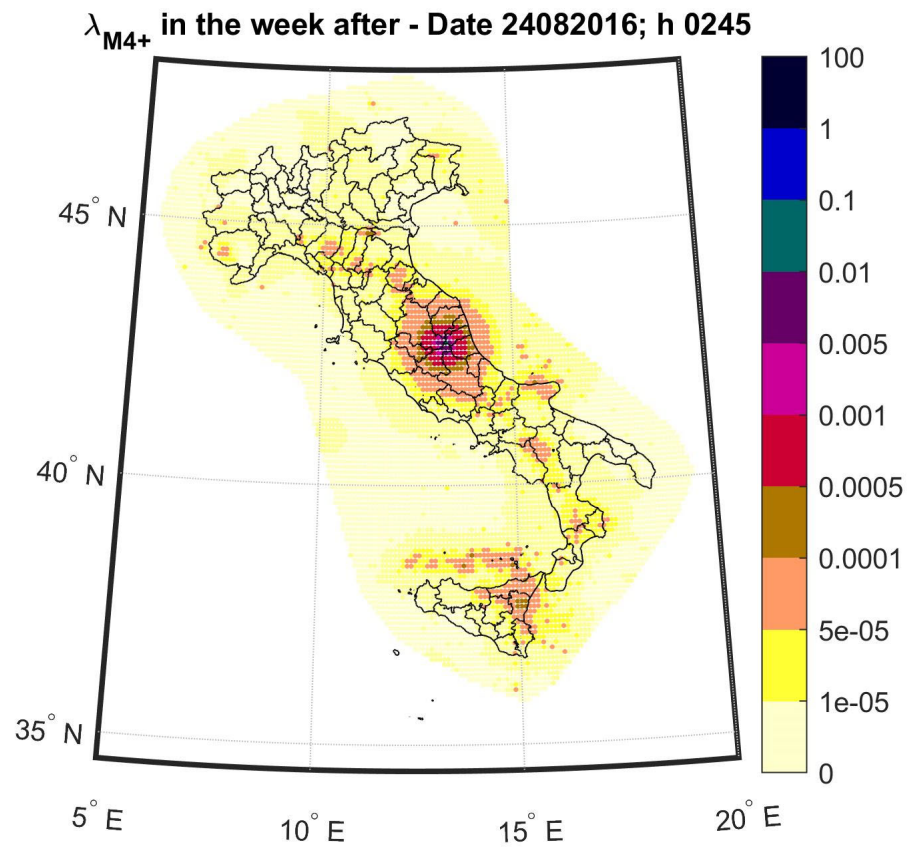
Figure 2. Weekly rates from OEF-Italy weekly at 24/08/2016, 02:45.
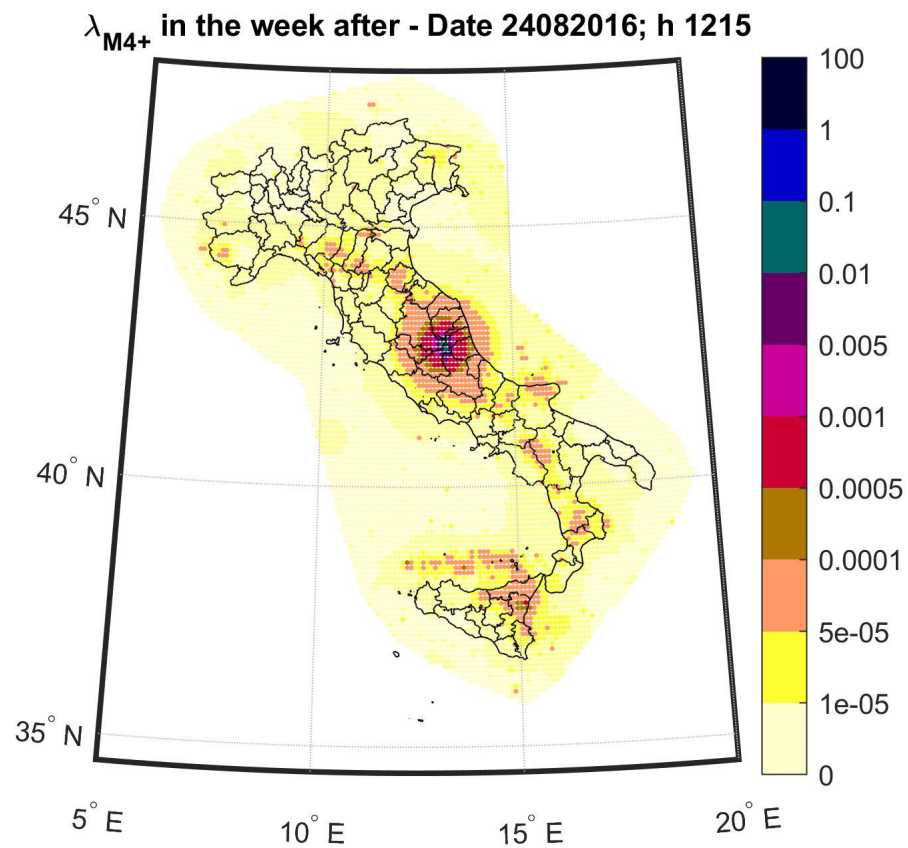
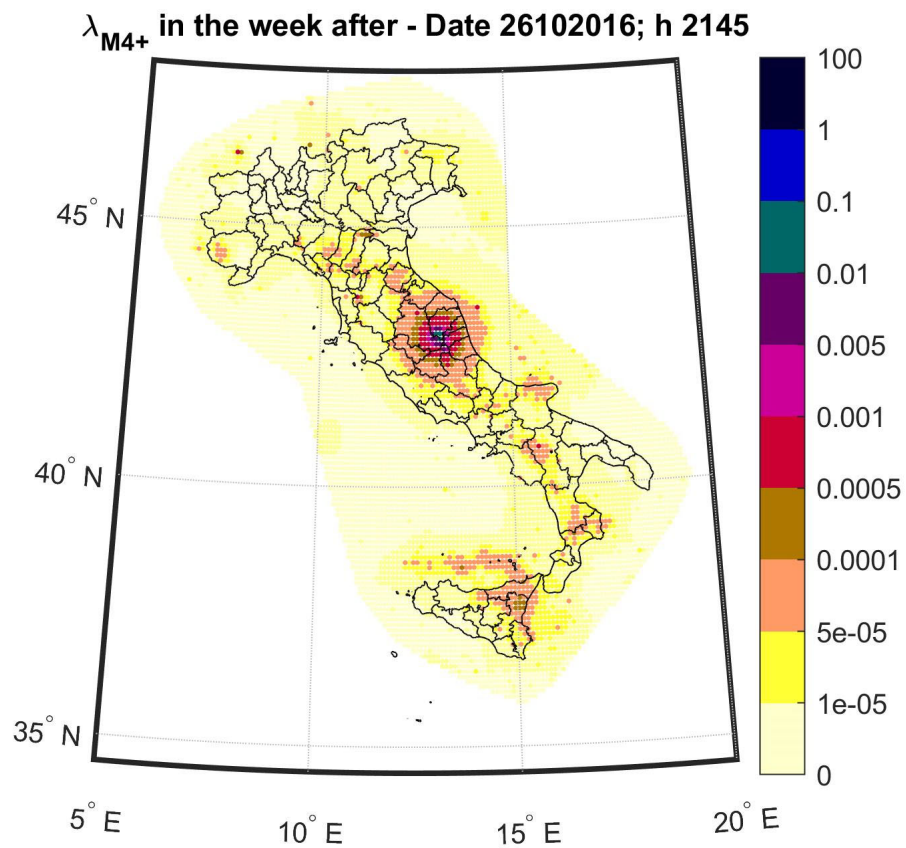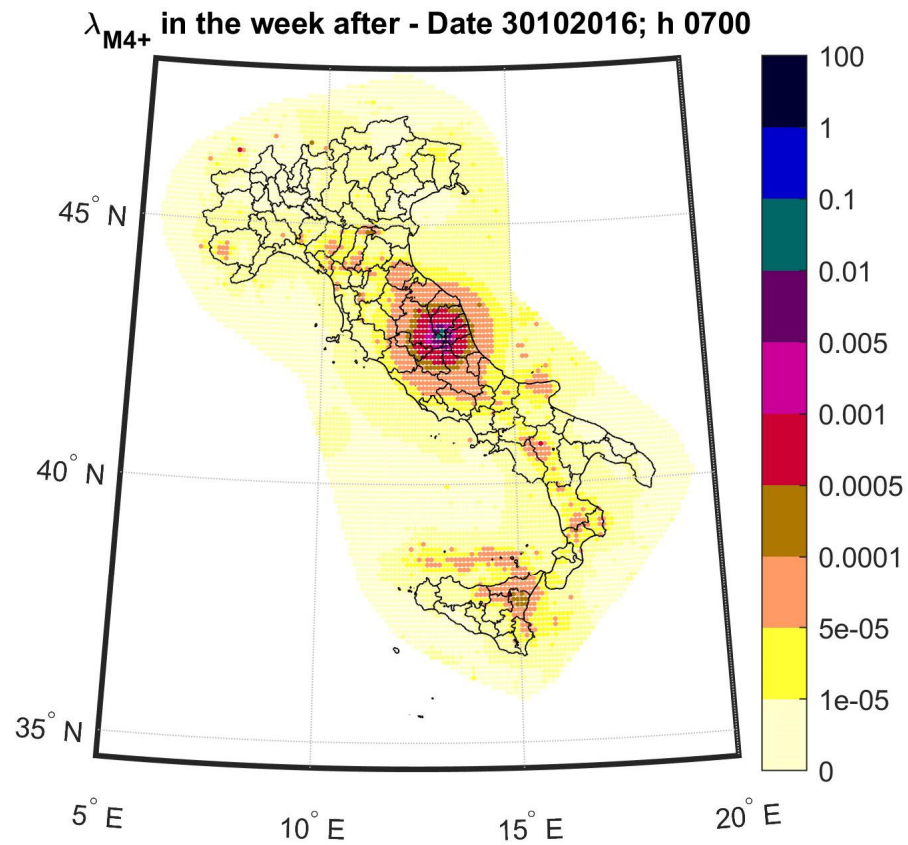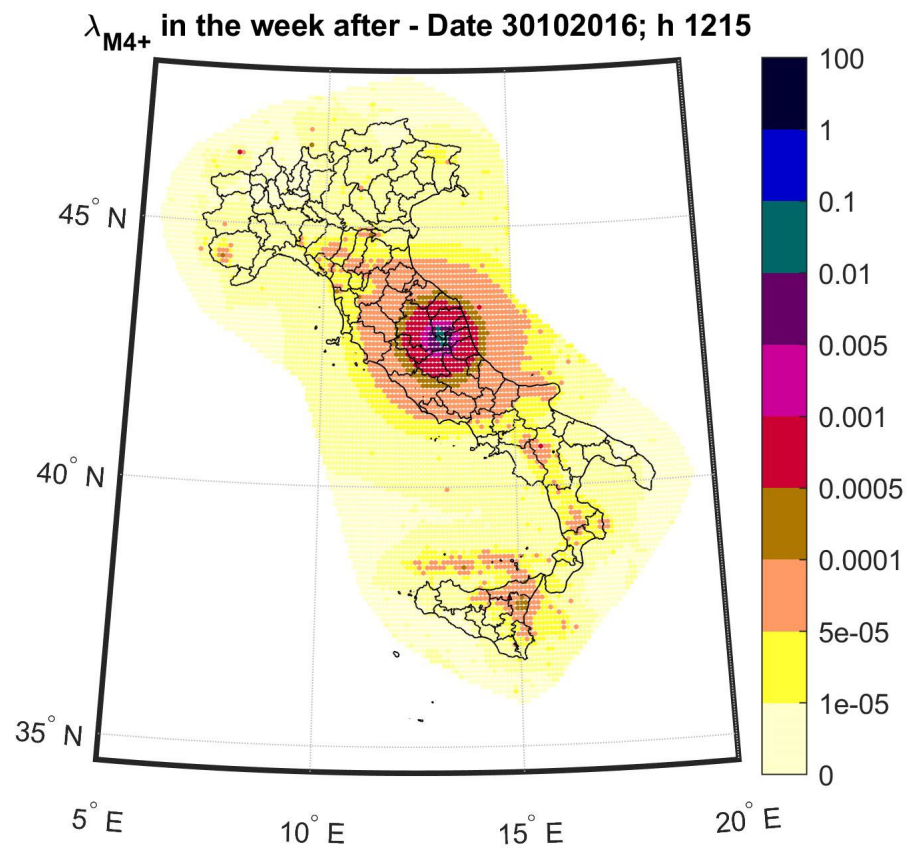**Figure 3. Weekly rates from OEF-Italy weekly at 24/08/2016, 12:15.**

λ_{M4+} **in the week after - Date 26082016; h 0445**
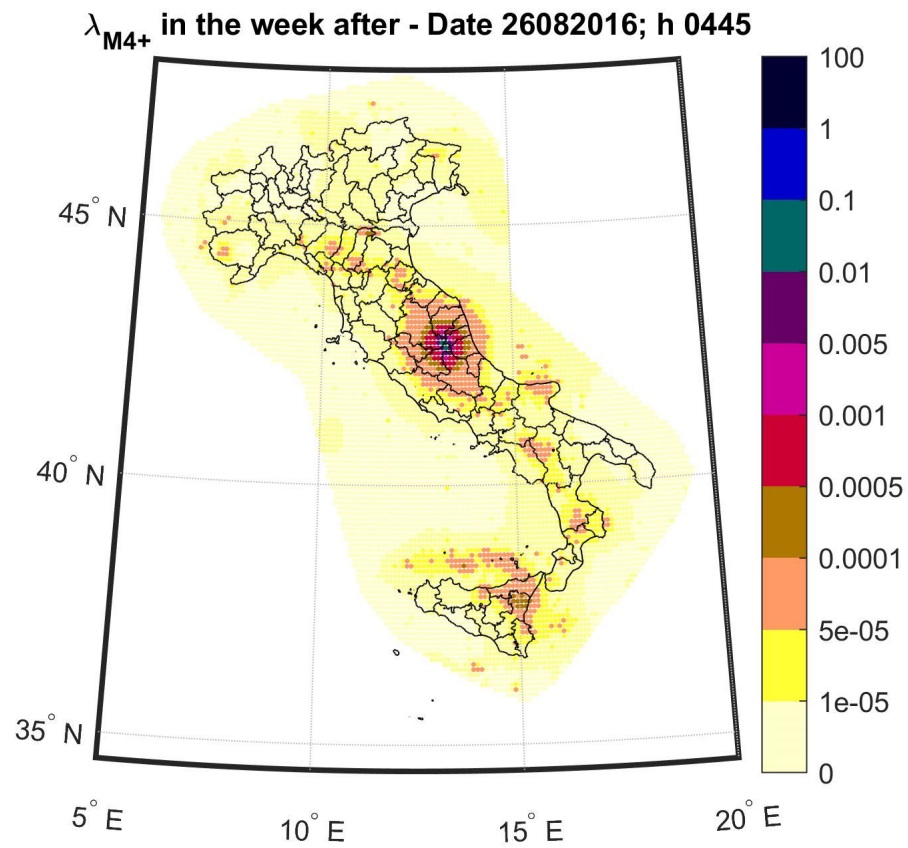
Figure 4. Weekly rates from OEF-Italy weekly at 26/08/2016, 04:45.

λ_{M4+} **in the week after - Date 26102016; h 1730**
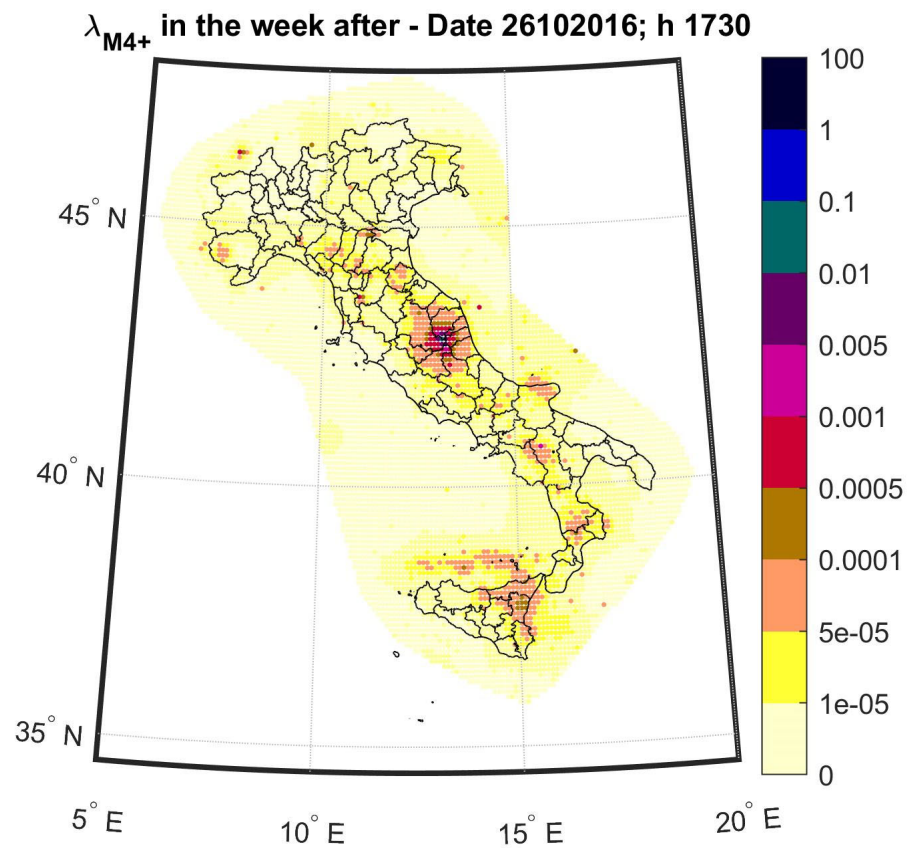
Figure 5. Weekly rates from OEF-Italy weekly at 26/08/2016, 17:30.

$\lambda_{\text{M4+}}$ **in the week after - Date 26102016; h 1930**
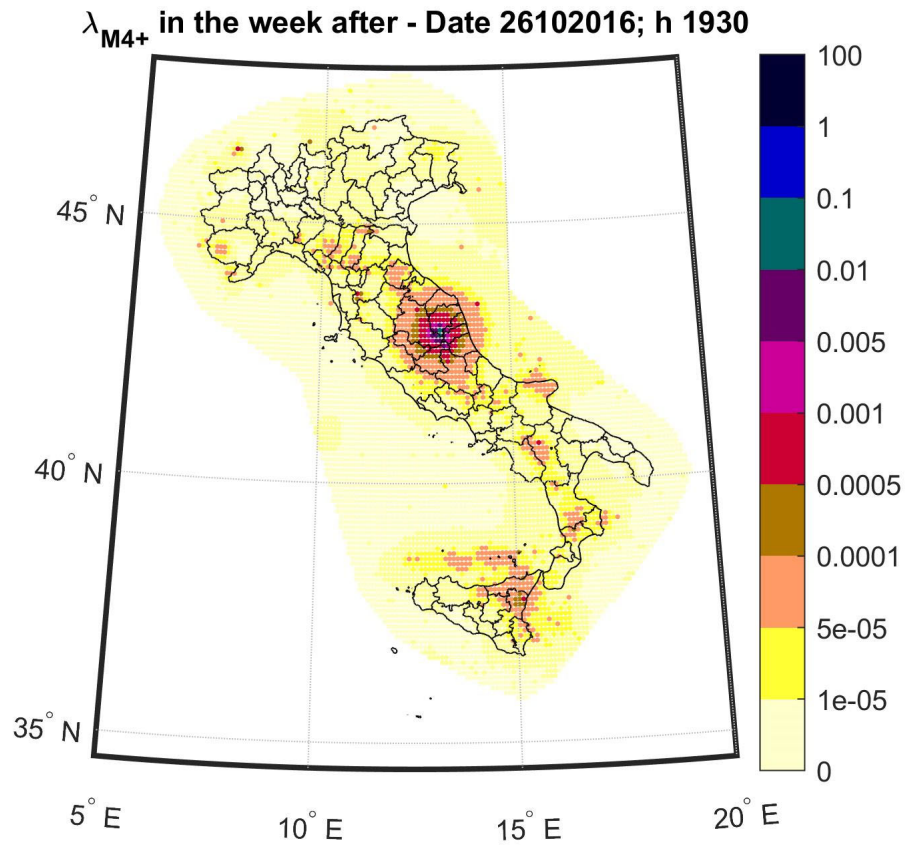
Figure 6. Weekly rates from OEF-Italy weekly at 26/10/2016, 19:30.

$\lambda_{\text{M4+}}$ **in the week after - Date 26102016; h 2145**

Figure 7. Weekly rates from OEF-Italy weekly at 26/10/2016, 21:45.

Figure 8. Weekly rates from OEF-Italy weekly at 30/10/2016, 07:00.

Figure 9. Weekly rates from OEF-Italy weekly at 30/10/2016, 12:15.
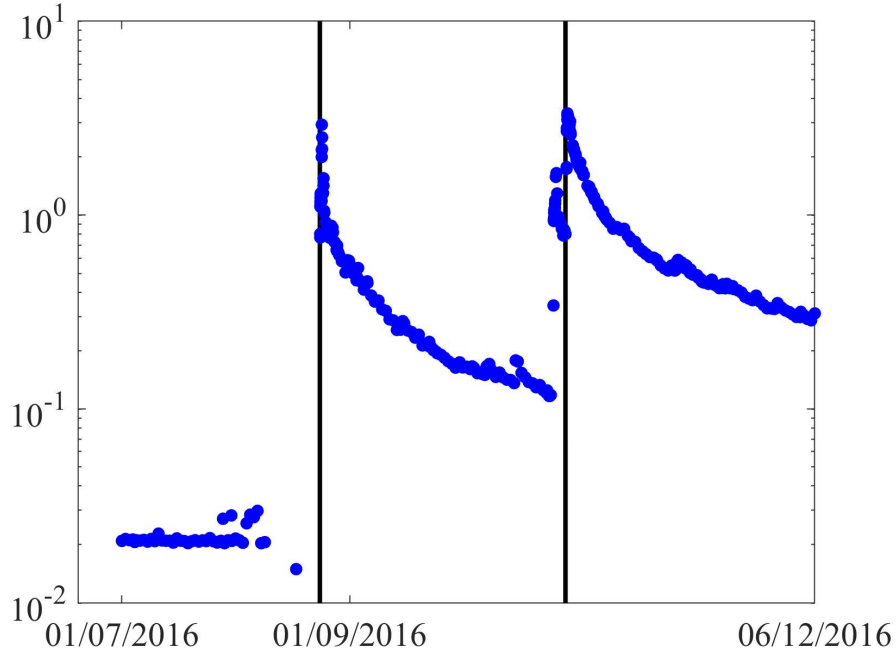
Figure 10. Sum of OEF rates for point-like source within 70 km from the epicenter of the mainshock; vertical lines are the dates of the M6 and M6.5 earthquakes.

The adopted state-dependent fragility functions are those developed in (Orlacchio et al., 2021) for each Italian structural typology and performance level. More specifically, five damage states were considered: undamaged (DS_0), slight damage (DS_1), moderate damage (DS_2), extensive damage (DS_3), and complete damage (DS_4). The adopted intensity measure is $Sa_{avg}(\mathbf{T})$ as defined in Eq. (6). As pertaining to exposure, for each Italian municipality, the number of the buildings of the k-th structural typology, N_B^k in Eq. (5), is in accordance with the results of the SERA project.

The $P[\theta_q]$ probability, adopted in Eq. (1), is computed, at the municipality scale, referring to the urbanized areas derived by the data of the *Italian Istituto Nazionale di Statistica* (ISTAT). More specifically, to compute $P[\theta_q]$, the grid of soil classes provided by (Forte et al., 2019) is super-imposed, to the map of urbanized areas. Thus, for each municipality, defining the total number of points within the urbanized areas, N_{urb}, and the number of points of a specific soil class, N_{θ_q}, $P[\theta_q]$ is computed as per Eq. (7), where $\theta_1, \theta_2, \theta_3, \theta_4$ correspond in turn to soil classes A, B, C, D of (Bindi et al., 2011) GMPE (an analogous procedure was adopted in (Pacifico et al., 2022):

$$P[\theta_q] = \frac{N_{\theta_q}}{N_{urb}}, \qquad q = \{1,...,4\}. \tag{7}$$

4. Results

This section summarizes the results provided by MANTIS v2.0. The forecasted percentage of buildings in each damage state are reported from Figure 11 to Figure 19 that refer to the OEF releases shown above. The considered municipalities are those for which INGV ShakeMaps were available.
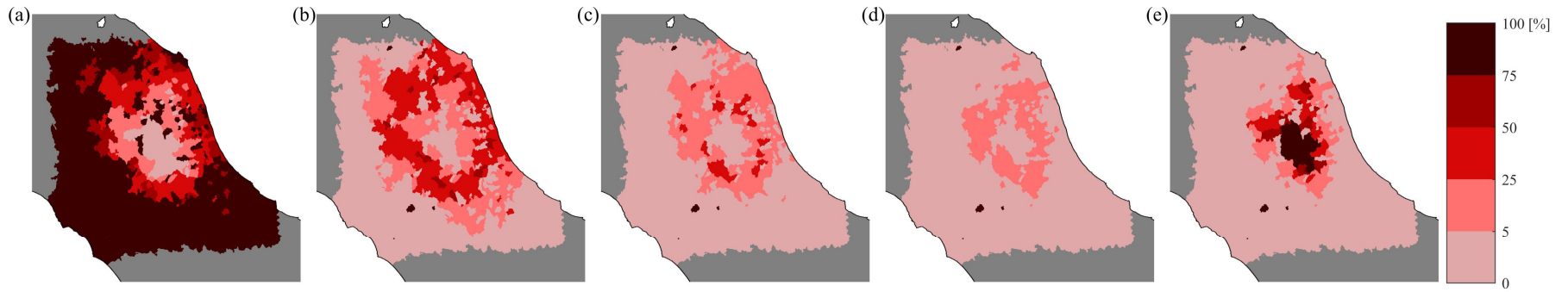
Figure 11. Expected percentage buildings per municipality in (a) DS_0, (b) DS_1, (c) DS_2, (d) DS_3, and (e) DS_4: Date of forecasting 24/08/2016, at 02:00.
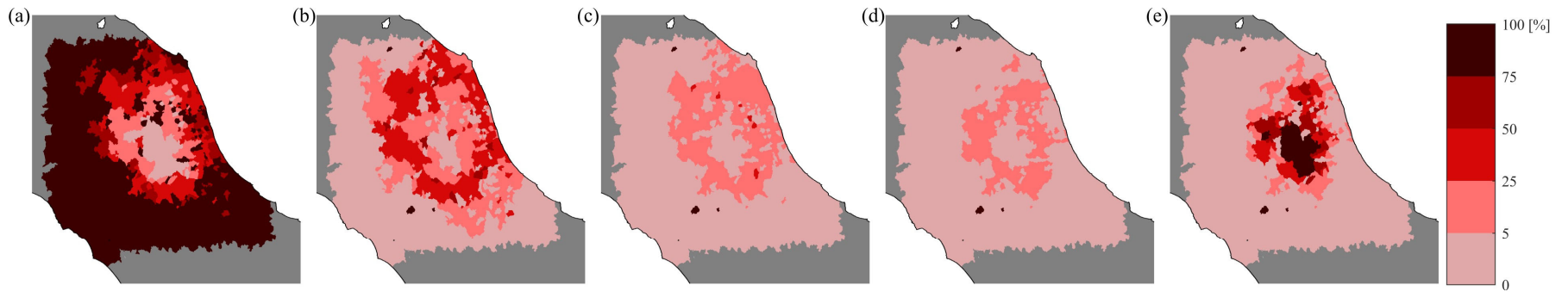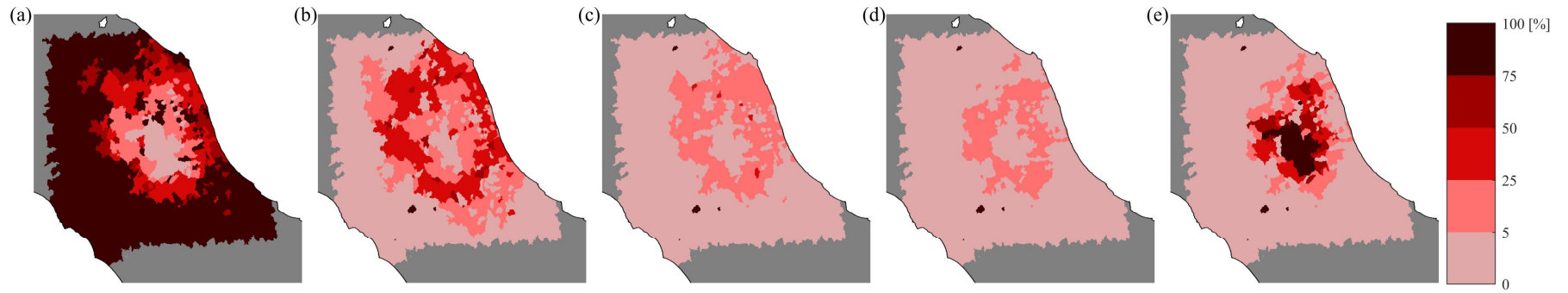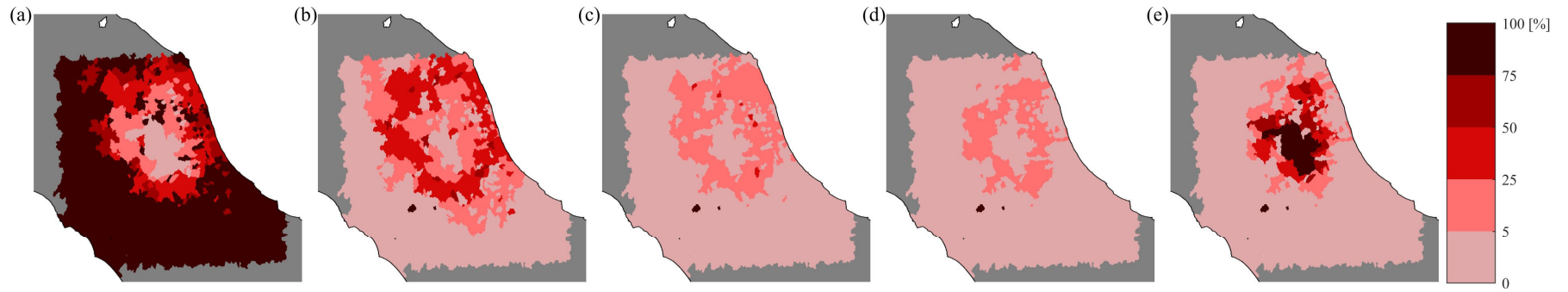

Figure 12. Expected percentage buildings per municipality in (a) DS_0, (b) DS_1, (c) DS_2, (d) DS_3, and (e) DS_4: Date of forecasting 24/08/2016, at 02:45.

Figure 13. Expected percentage buildings per municipality in (a) DS_0, (b) DS_1, (c) DS_2, (d) DS_3, and (e) DS_4: Date of forecasting 24/08/2016, at 12:15.

Figure 14. Expected percentage buildings per municipality in (a) DS_0, (b) DS_1, (c) DS_2, (d) DS_3, and (e) DS_4: Date of forecasting 26/08/2016, at 04:45.
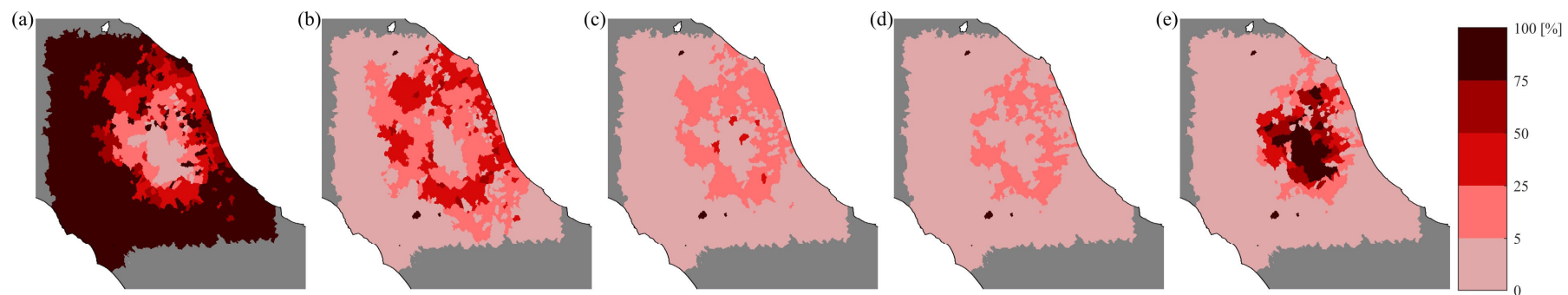
Figure 15. Expected percentage buildings per municipality in (a) DS_0, (b) DS_1, (c) DS_2, (d) DS_3, and (e) DS_4: Date of forecasting 26/10/2016, at 17:30.
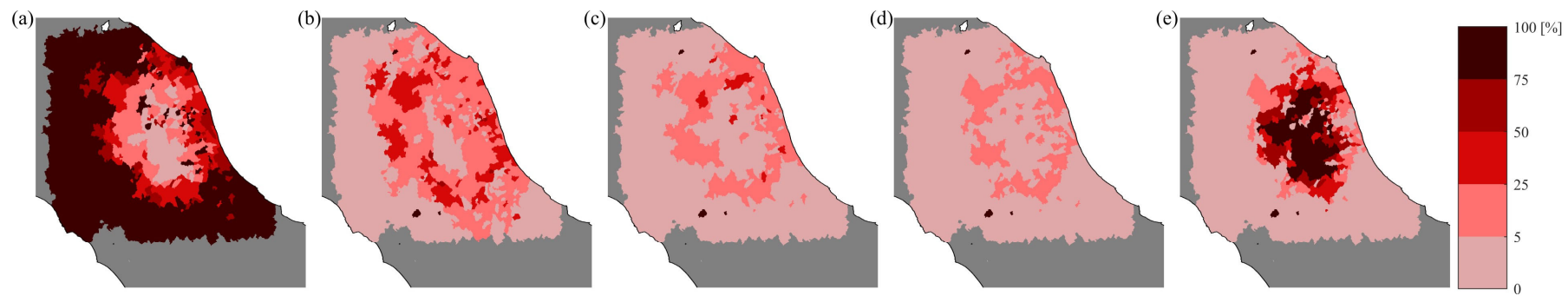

Figure 16. Expected percentage buildings per municipality in (a) DS_0, (b) DS_1, (c) DS_2, (d) DS_3, and (e) DS_4: Date of forecasting 26/10/2016, at 19:30.
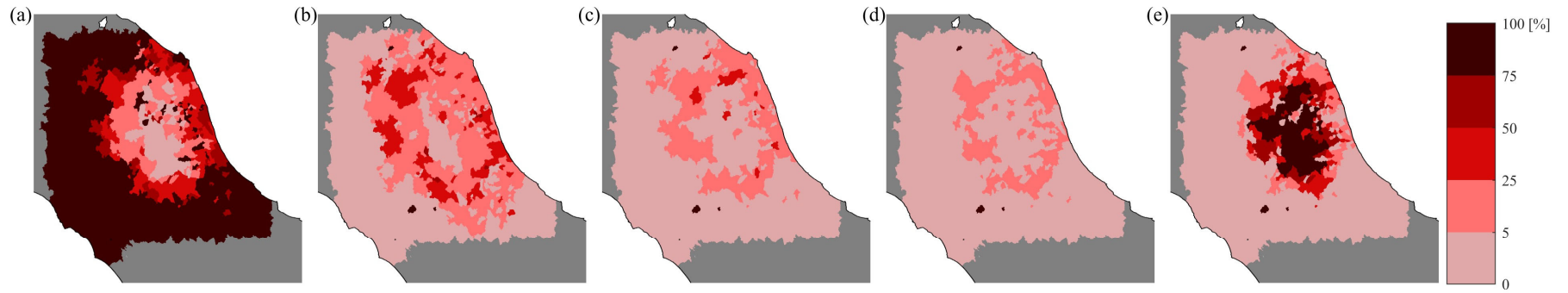
Figure 17. Expected percentage buildings per municipality in (a) *DS$_0$*, (b) *DS$_1$*, (c) *DS$_2$*, (d) *DS$_3$*, and (e) *DS$_4$*: Date of forecasting 26/10/2016, at 21:45.

Figure 18. Expected percentage buildings per municipality in (a) *DS$_0$*, (b) *DS$_1$*, (c) *DS$_2$*, (d) *DS$_3$*, and (e) *DS$_4$*: Date of forecasting 30/10/2016, at 07:00.
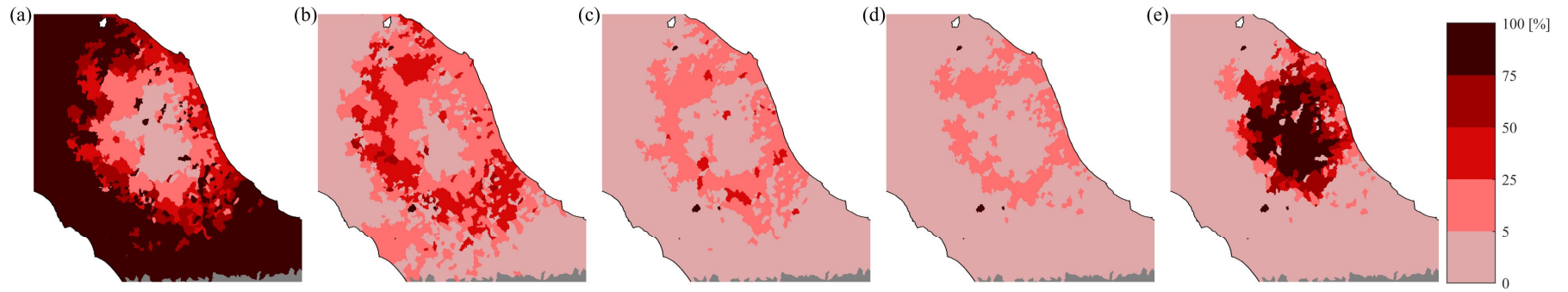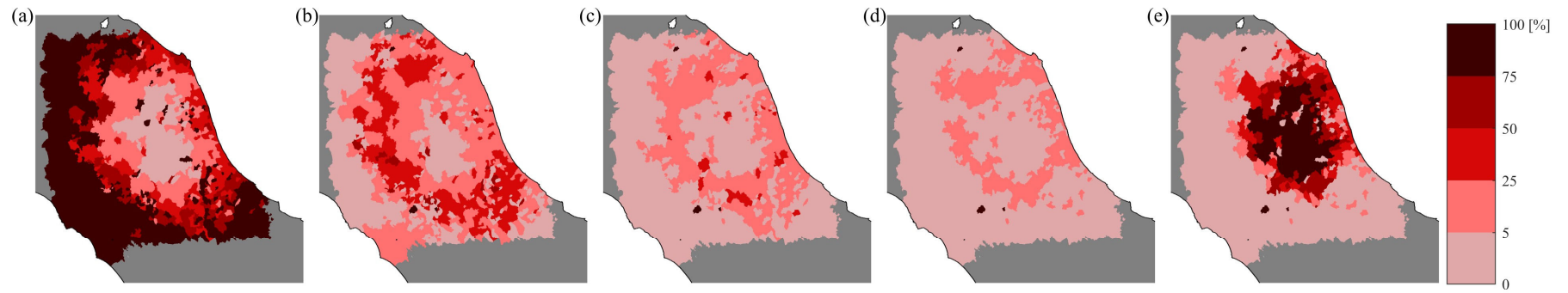
Figure 19. Expected percentage buildings per municipality in (a) DS_0, (b) DS_1, (c) DS_2, (d) DS_3, and (e) DS_4: Date of forecasting 30/10/2016, at 12:15.

The figures show that, during the evolution of the seismic sequence, the buildings of the munici-palities most affected by the earthquakes move from the undamaged conditions to the DS_4.

Figure 20 summarizes the damage evolution showing the percentage of buildings in each damage state for all the municipalities considered in the preceding figures. As shown, the first forecasting provides about 80% of the buildings in the undamaged conditions: this account for the estimated damage produced by the M6 and M4.5 earthquake occurred at 01:36 and 01:37 (see Table 1) and the forecasted damages in accordance with OEF rates released at 02:00. In the last forecast, the expected percentage of buildings in undamaged conditions are about 60% and those in complete damage conditions are less than 20%.
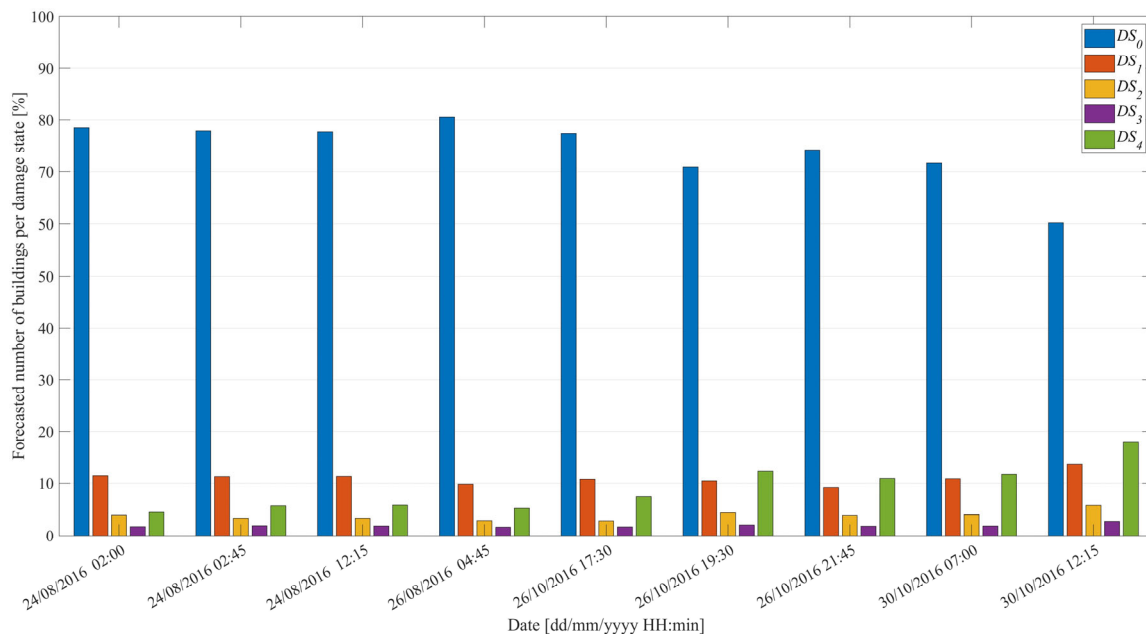

Figure 20. Expected percentage buildings in each damage state for the whole geographic area.

5.   CONCLUSIONS

MANTIS-K, an Italian system for operational earthquake loss forecasting, was formulated to con-vert the weekly seismic rates provided by an operational earthquake forecasting system into weekly seismic risk metrics. During the RISE project, an upgraded version of MANTIS-K, MANTIS v2.0, was formulated to overcome some limitations of the first OELF system. Thus, MANTIS v2.0 is now able to account for the evolution of structural damage due to subsequent earthquakes.

To demonstrate the potentialities of MANTIS v2.0, the Central Italy 2016 seismic sequence was analyzed and results were provided in this deliverable.

6.   References

Baker, J. W., & Cornell, C. A. (2006). Spectral shape, epsilon and record selection. *Earthquake Engineering & Structural Dynamics*, *35*(9), 1077–1095. https://doi.org/10.1002/eqe.571

Bindi, D., Pacor, F., Luzi, L., Puglia, R., Massa, M., Ameri, G., & Paolucci, R. (2011). Ground motion prediction equations derived from the Italian strong motion database. *Bulletin of Earthquake Engineering*, *9*(6), 1899–1920. https://doi.org/10.1007/s10518-011-9313-z

Chioccarelli, E., Pacifico, A., & Iervolino, I. (2023). *Operational earthquake loss forecasting for Europe, RISE Project Deliverable 4.3.*

Forte, G., Chioccarelli, E., de Falco, M., Cito, P., Santo, A., & Iervolino, I. (2019). Seismic soil classification of Italy based on surface geology and shear-wave velocity measurements. *Soil Dynamics and Earthquake Engineering*, *122*(3), 79–93. https://doi.org/10.1016/j.soildyn.2019.04.002

Gutenberg, B., & Richter, C. F. (1944). Frequency of earthquakes in California. *Bulletin of the Seismological Society of America*, *34*(4), 185–188. https://doi.org/10.1785/bssa0340040185

Iervolino, I., Baltzopoulos, G., Chioccarelli, E., & Suzuki, A. (2017). Seismic actions on structures in the near-source region of the 2016 central Italy sequence. *Bulletin of Earthquake Engineering*, 1–19. https://doi.org/10.1007/s10518-017-0295-3

Iervolino, I., Chioccarelli, E., Giorgio, M., Marzocchi, W., Zuccaro, G., Dolce, M., & Manfredi, G. (2015). Operational (short-term) earthquake loss forecasting in Italy. *Bulletin of the Seismological Society of America*, *105*(4), 2286–2298. https://doi.org/10.1785/0120140344

Iervolino, I., Giorgio, M., & Chioccarelli, E. (2016). Markovian modeling of seismic damage accumulation. *Earthquake Engineering and Structural Dynamics*, *45*(3), 441–461. https://doi.org/10.1002/eqe.2668

Jordan, T. H., Chen, Y. T., Gasparini, P., Madariaga, R., Main, I., Marzocchi, W., Papadopoulos, G., Sobolev, G., Yamaoka, K., & Zschau, J. (2011). Operational earthquake forecasting: State of knowledge and guidelines for utilization. *Annals of Geophysics*, *54*(4), 319–391. https://doi.org/10.4401/ag-5350

Luzi, L., Pacor, F., Puglia, R., Lanzano, G., Felicetta, C., Amico, M. D. ', Michelini, A., Faenza, L., Lauciani, V., Iervolino, I., Baltzopoulos, G., & Chioccarelli, E. (2017). The Central Italy Seismic Sequence between August and December 2016: Analysis of Strong-Motion Observations. *Seismological Research Letters*, *88*, 1219–1231. https://doi.org/10.1785/0220170037

Marzocchi, W., Lombardi, A. M., & Casarotti, E. (2014). The establishment of an operational earthquake forecasting system in Italy. *Seismological Research Letters*, *85*(5), 961–969. https://doi.org/10.1785/0220130219

Orlacchio, M., Chioccarelli, E., Baltzopoulos, G., & Iervolino, I. (2021). State-Dependent Seismic Fragility Functions for Italian Reinforced Concrete Structures: Preliminary Results. *31th European Safety and Reliability Conference, 19-23 September 2021, Angers, France*, 1591–1598. https://doi.org/10.3850/978-981-18-2016-8_660-cd

Pacifico, A., Chioccarelli, E., & Iervolino, I. (2022). Residential code-conforming structural seismic risk maps for Italy. *Soil Dynamics and Earthquake Engineering*, *153*, 1–13. https://doi.org/10.1016/j.soildyn.2021.107104

Liability Claim

The European Commission is not responsible for any that may be made of the information contained in this document. Also, responsibility for the information and views expressed in this document lies entirely with the author(s).